Title: A Thermodynamic Evaluation of Antibody-Surface Interactions in Multimodal Cation Exchange Chromatography

Authors: Ronak B. Gudhka[1], David J. Roush[2], Steven M. Cramer[1]

Affiliations: [1]Howard P. Isermann Department of Chemical and Biological Engineering and Center for Biotechnology and Interdisciplinary Studies, Rensselaer Polytechnic Institute, 110 Eighth Street, Troy, New York 12180, United States
[2]Biologics Process R&D, Merck Co., Inc., 2000 Galloping Hill Road, Kenilworth, New Jersey 07033, United States

Corresponding Author: Dr. Steven M. Cramer

Corresponding Author's affiliations: Dept. of Chemical and Biological Engineering and Center for Biotechnology and Interdisciplinary Studies, Rensselaer Polytechnic Institute, 110 Eighth Street, Troy, New York 12180, United States

Corresponding Author's Email: crames@rpi.edu

Corresponding Author's telephone number: 518-276-6198

A Thermodynamic Evaluation of Antibody-Surface Interactions in Multimodal Cation Exchange Chromatography

Ronak B. Gudhka[1], David J. Roush[2], Steven M. Cramer[1]

[1]Howard P. Isermann Department of Chemical and Biological Engineering and Center for Biotechnology and Interdisciplinary Studies, Rensselaer Polytechnic Institute, 110 Eighth Street, Troy, New York 12180, United States
[2]Biologics Process R&D, Merck Co., Inc., 2000 Galloping Hill Road, Kenilworth, New Jersey 07033, United States

1 Abstract

In this study, the thermodynamics of binding of two industrial mAbs to multimodal cation exchange systems was investigated over a range of buffer and salt conditions via a van't Hoff analysis of retention data. Isocratic chromatography was first employed over a range of temperature and salt conditions on three multimodal resins and the retention data were analyzed in both the low and high salt regimes. While mAb retention decreased with salt for all resins at low salts, retention increased at high salts for two of the resins, suggesting a shift from electrostatic to more hydrophobic driven interactions. The retention data at various temperatures were then employed to generate non-linear van't Hoff plots which were fit to the quadratic form of the van't Hoff equation. At low salts, retention of both mAbs decreased with increasing temperature and the van't Hoff plots were concave downward on Capto MMC and Nuvia cPrime, while being concave upward on Capto MMC ImpRes. Different trends were observed on some of the resins with respect to both the concavity of the van't Hoff plots as well as the impact of temperature on the favorable enthalpies in the low salt regime. Interestingly, while increasingly favorable enthalpy with temperature was observed with Capto MMC and Nuvia cPrime at low salt, favorable enthalpy decreased with temperature for Capto MMC ImpRes. At high salts, binding of both mAbs on the two Capto resins were consistently entropically driven, consistent with desolvation. While the negative heat capacity data at low salts indicated that desolvation of polar/charged groups were important in Capto MMC and Nuvia cPrime, the positive data suggested that desolvation of non-polar groups were more important with Capto MMC ImpRes. Finally, the data at high salts indicated that desolvation of non-polar groups was the major driver for binding of both mAbs to the Capto resins under these conditions.

Key words: Multimodal chromatography, thermodynamics, non-linear van't Hoff plot, monoclonal antibody.

2 Introduction

Traditional platform processes for the downstream purification of monoclonal antibodies (mAbs) have employed post protein A polishing steps that have used single mode interaction systems such as ion exchange (IEX) or hydrophobic interaction chromatography (HIC) [1,2]. Recently, multimodal (MM) chromatography has emerged as a promising alternative polishing step owing to enhanced selectivity resulting from the combination of electrostatic, hydrogen bonding, hydrophobic and/or aromatic interactions within a single ligand [3–8]. Further, MM resin materials that vary in surface properties (e.g. geometric presentation of functional groups, ligand density, linker between resin and ligand) have been shown to interact differently with libraries of model proteins thus creating unique windows of selectivity as compared to the traditional single mode interaction systems [9–12].

Our group and several others have been actively working on improving our understanding of selectivity in MM chromatography [9–29]. Chung et al. employed a library of cold shock protein B mutant variants to demonstrate the importance of charge and hydrophobicity on the protein surface for interacting with MM chromatographic systems [13]. Nfor et al. developed an empirical mixed mode isotherm to model the binding of proteins to MM resins [24]. Tong et al. have employed Molecular Dynamics (MD) simulations to provide a molecular level understanding of the mechanisms involved in the binding of the IgG1-F_C domain to a hydrophobic charge induction chromatographic (HCIC) system at different pH and ligand densities [29]. Woo et al. and Robinson et al. have examined the retention of a library of model proteins to shed light on the effect of ligand structure, chemistry and density on selectivity patterns observed in MM cation exchange (MM CEX) and anion exchange (MM AEX) systems [11,12]. Srinivasan et al. have used biophysical techniques (Nuclear Magnetic Resonance (NMR), Atomic Force Microscopy (AFM), Isothermal Titration Calorimetry (ITC)) in combination with Molecular Dynamics (MD) simulations to study the binding of a preferred face of ubiquitin on two MM CEX surfaces; Capto MMC and Nuvia cPrime [22,23]. Robinson et al. have also examined potential preferred binding regions of mAbs in MM CEX systems [16]. While these and other studies have improved our understanding of protein-surface interactions in MM systems, there is still a lack of understanding of the thermodynamic basis of these interactions, especially for large complex biomolecules like mAbs.

There is a vast literature that has employed a van't Hoff (VH) analysis of chromatographic retention data to study the thermodynamics [30–39]. Roush et al. used linear VH plots to evaluate the effect of temperature on the binding of recombinant rat cytochrome b_5 to an AEX resin [30]. While linear VH plots are associated with a zero heat capacity change ($\Delta C_{P,ads}$), these plots are often non-linear, indicating a heat capacity change (either positive or negative) associated with binding. Thus, protein chromatography often requires a non-linear VH analysis in order to fully describe the behavior. This has been carried out using either a logarithmic approach which assumes the heat capacity change to be temperature invariant or a quadratic formulation that allows for variation of $\Delta C_{P,ads}$ with temperature [31]. Several groups have employed these non-linear VH analyses to elucidate the mechanisms of protein binding in various single mode interaction systems such as HIC and IEX. In the current study, we employ the quadratic formulation of the VH equation to examine how the enthalpic and entropic contributions to binding change with mAb and salt concentration in different MM CEX chromatographic systems.

In the current paper, MM chromatographic separations that have previously been reported to exhibit interesting selectivity trends for two commercial mAbs are examined from a thermodynamic perspective. Isocratic retention of these mAbs on three commercial MM CEX resins (Capto MMC, Nuvia cPrime and Capto MMC ImpRes) is carried out over a range of salt and temperature conditions and a quadratic Van't Hoff analysis is carried out to determine the enthalpic and entropic contributions as well as the heat capacity changes associated with these interactions at low and high salt regimes. The work presented in this paper provides thermodynamic insights into mAb binding in MM CEX chromatography.

3 Materials and Methods

3.1 Materials

Purified IgG1 antibodies (A, pI 7.59 and C, pI 8.27) were supplied by Merck and Co., Inc. (Kenilworth, NJ, 07033, USA). Both the antibodies have a common F_C domain but have different Fab domains as identified by the amino acid sequence. Disposable PD10 desalting columns were purchased from Cytiva (Uppsala, Sweden). Sodium acetate, Tris base, sodium chloride and hydrochloric acid were purchased from Sigma-Aldrich (St. Louis, MO, 63134, USA). Capto™ MMC and Capto™ MMC ImpRes chromatographic resins were purchased from Cytiva (Uppsala,

Sweden). Nuvia™ cPrime™ chromatographic resin was donated by Bio-Rad Laboratories (Hercules, CA, 94547, USA).

3.2 Protein Solutions

Protein solutions were buffer exchanged using the PD10 desalting columns. Briefly, the column was equilibrated with buffer B (20 mM sodium acetate, Tris and 2.5 M NaCl adjusted to pH 6.0). 2.5 mL of protein sample (~10 mg/mL) was added to the column and the buffer was allowed to flow through. The buffer exchanged protein was eluted by addition of 3.5 mL of buffer B and was diluted with appropriate amounts of buffer A (20 mM sodium acetate, Tris adjusted to pH 6.0) to get the desired salt concentration as well as a final mAb concentration of 3 mg/mL.

3.3 Chromatography Experiments

Chromatographic media were packed into a 5 x 50 mm column and isocratic chromatography was carried out at 1 column volume (CV)/min on an ÄKTA™ Explorer 100 (Cytiva, Uppsala, Sweden) controlled by Unicorn 5.1 software (except 4°C experiments, which were performed on ÄKTA™ prime). Experiments were conducted in a temperature-controlled room maintained at different temperatures (4°C, 17°C, 22°C, 30°C and 37°C ± 0.5°C). Buffers A and B (described above) were used for all the experiments and columns were regenerated using 1 M sodium hydroxide to prepare the columns for the next protein injection. The column was equilibrated at the desired salt concentration by appropriately mixing buffers A and B followed by injection of 100 µL of buffer exchanged protein (3 mg/mL) in the running buffer. The column effluent was monitored at a UV wavelength of 280 nm. An acetone pulse was used to determine the retention time of an inert unretained solute. Retention time was determined by the average first moment from duplicate runs.

4 Theory

The retention factor was determined directly from the chromatogram as [40]:

$$k' = \frac{t_R - t_0}{t_0} \tag{1}$$

where t_R is the retention time of the solute and t_0 is the retention time of an inert unretained solute. The phase ratio was determined using the retention time of the unretained solute [41]

$$\emptyset = \frac{V - t_0 V'}{t_0 V'} \quad (2)$$

where V is the column volume and V′ is the volumetric flowrate. It is important to note that this definition of the phase ratio considers the entire volume of the resin to be the stationary phase volume ($V - t_0 V'$), consistent with the previous literature [30–39].

The thermodynamic framework presented here is adopted from ref [31]. The relationship between the retention factor and the equilibrium constant is given by:

$$k' = K_{eq}\emptyset \quad (3)$$

The Gibbs free energy of adsorption is linearly related to the logarithm of the equilibrium rate constant as follows:

$$\Delta G_{ads} = -RTlnK_{eq} \quad (4)$$

where R is universal gas constant and T is the absolute temperature. Combining equations 3 and 4 along with the standard thermodynamic formulations, we obtain the linear VH equation:

$$lnk' = \frac{-\Delta H_{ads}}{RT} + \frac{\Delta S_{ads}}{R} + ln\emptyset \quad (5)$$

where ΔH_{ads} and ΔS_{ads} are the enthalpy and entropy changes for adsorption. This equation holds true only when the heat capacity change is zero and the enthalpy and entropy changes are independent of temperature. When the heat capacity changes for adsorption to chromatographic resins are non-zero and non-constant, the resulting non-linear quadratic VH equation is obtained:

$$lnk' = a + \frac{b}{T} + \frac{c}{T^2} + ln\emptyset \quad (6)$$

The parameters a, b and c can be calculated by fitting equation 6 to the experimental data and equations 7, 8 and 9 can then be used to determine the enthalpic and entropic contributions and the heat capacity change upon adsorption.

$$\Delta H_{ads} = -R\left(b + \frac{2c}{T}\right) \quad (7)$$

$$\Delta S_{ads} = R\left(a - \frac{2Rc}{T^2}\right) \quad (8)$$

$$\Delta C_{p,ads} = \frac{2Rc}{T^2} \quad (9)$$

5 Results and Discussion

5.1 Linear Gradient Chromatography

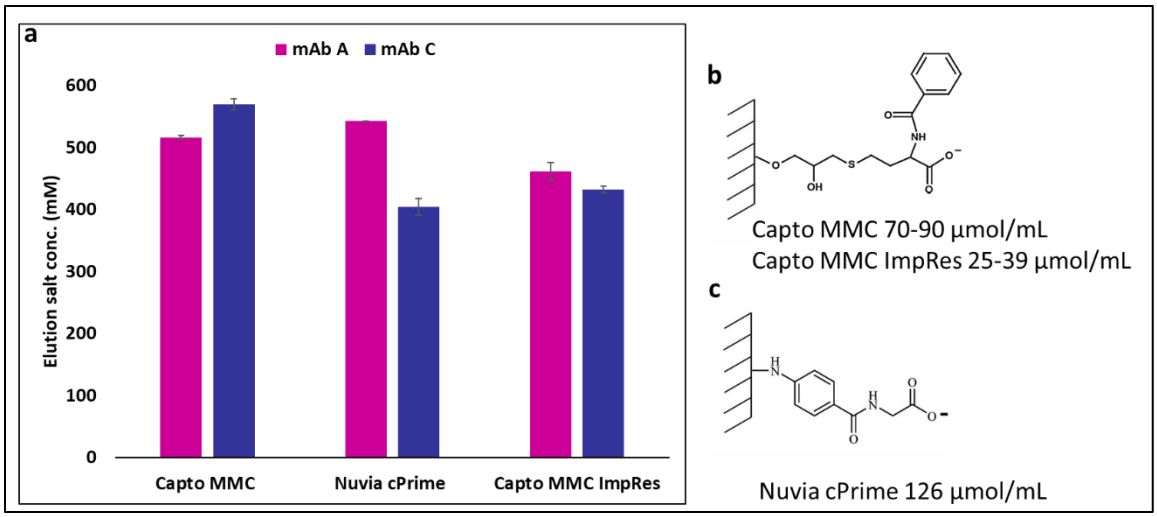

Figure 1. (a) Chromatographic retention of mAbs A (purple) and C (blue) on multimodal cation exchange chromatography systems and structures of the (b) Capto and (c) Nuvia cPrime ligand head groups (numbers in parenthesis indicate the corresponding ligand densities on the chromatographic resin surfaces). Capto MMC and Capto MMC ImpRes resins have the same ligand head group with different surface ligand density. Linear salt gradients were from 0 to 1 M NaCl, 40 column volumes, pH 6. Retention data reproduced from ref [16].

Our group has previously reported that two mAbs exhibited different selectivity patterns on three commercially available MM CEX resins (Capto MMC, Nuvia cPrime, Capto MMC ImpRes) [16]. These two mAbs shared a common F_C with different Fab domains resulting in pIs of 7.6 and 8.3 for mAbs A and C, respectively. The MM ligands in these resins are shown in Figure 1, with the aromatic ring being more solvent exposed for the Capto MMC ligand (Figure 1b) as compared to the Nuvia cPrime ligand (Figure 1c). In addition, while the Capto MMC and Nuvia cPrime resins had relatively high ligand densities the Capto MMC Impress had significantly lower density. As can be seen in Figure 1a (data obtained from Figure 6 of ref [16]) the elution order on Capto MMC (mAb A followed by mAb C) was different than that observed in Nuvia cPrime and Capto MMC ImpRes. While the selectivity difference between Capto MMC and Nuvia cPrime was mainly due to the higher retention of mAb C on Capto MMC, the shift in selectivity in Capto MMC ImpRes was more subtle with both mAbs exhibiting reduced binding. In order to study the

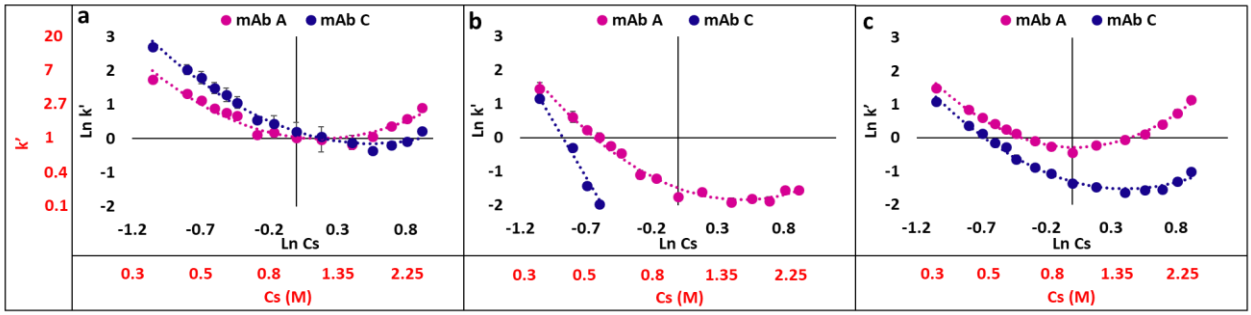

Figure 2. Ln k' vs Ln Cs plots for retention of mAbs A (purple) and C (blue) on (a) Capto MMC, (b) Nuvia cPrime and (c) Capto MMC ImpRes at room temperature (295 K).

relative electrostatic and hydrophobic behavior of these systems, we first examined the impact of salt on the retention behavior of these mAbs in the three resin systems at room temperature.

5.2 Isocratic Chromatography

As described in methods section, isocratic chromatography experiments were carried out with mAbs A and C on Capto MMC, Nuvia cPrime and Capto MMC ImpRes at different salt concentrations ranging from 0.45 M to 2.5 M NaCl. The retention times of the mAbs (first moment) at a given condition were used for calculating the k's and the resulting ln-ln plots for mAbs A and C on these resins at room temperature (22°C) are presented in Figure 2. To facilitate the discussion, we divide the salt concentration range into the low salt (below 1.2 M NaCl) and high salt regimes (1.2 to 2.5 M NaCl). In the low salt regime, the elution order observed in the isocratic experiments was in qualitative agreement with that seen in the linear salt gradient experiments (Figure 1a) on all resin systems. Further, in this regime the retention of both mAbs decreased with increasing salt concentrations. In this salt range, both mAbs were more retained on Capto MMC and Capto MMC ImpRes as compared to Nuvia cPrime. Interestingly, the decrease in retention with salt observed in the Nuvia resin was significantly more pronounced than that seen with the Capto resins, indicating that while electrostatic interactions were likely playing a dominant role in Nuvia cPrime the interactions in the Capto systems were more complex. It can also be seen that the Capto MMC system had higher retention and selectivity than the Capto MMC ImpRes system at low salt conditions. This is likely due to the enhanced electrostatic interactions occurring at higher ligand densities [42].

This difference in elution behavior on these resin systems was even more pronounced at elevated salt conditions. For the Nuvia system, while mAb C was not retained in this high salt regime, there was a very weak retention of mAb A that plateaued with increasing salt

concentration. In contrast, the retention of the mAbs increased in both Capto systems at the higher salt concentrations. Further, while the retention plots were similar for mAb A at both ligand densities, the behavior of mAb C was markedly different on the Capto MMC and Capto MMC ImpRes systems.

At elevated salt concentrations, electrostatic interactions are screened, and hydrophobic interactions tend to play a more dominant role. The difference in retention behavior between the Nuvia cPrime and the Capto systems is likely due to the enhanced hydrophobicity of the Capto ligand which has the more solvent exposed aromatic ring [10]. This has also been observed previously when examining a range of model proteins [10,11]. Previous work on the chromatographic behavior of mAbs A and C in HIC systems and their surface hydrophobicities using a Surface Aggregation Propensity (SAP) analysis have established that mAb A is more hydrophobic [16]. Thus, at elevated salt concentrations, it would be expected that mAb A would have a higher retention than mAb C on a ligand with higher relative hydrophobic properties. Further, the dramatic difference in the retention behavior of mAb C at elevated salt concentrations in the Capto MMC and Capto MMC ImpRes systems is likely due to the decreased hydrophobicity of the lower ligand density Capto MMC ImpRes system. This may also be related to the recently hypothesized aromatic cluster behavior at the higher ligand density, which may further enhance the degree of hydrophobic interactions with mAb C [19].

These results indicate that very different retention behavior occurred with these two mAbs in three MM systems at various salt conditions. Since the retention mechanisms in multimodal chromatography can be quite complex, with many modes of interactions playing a role, we carried out a VH analysis to determine the thermodynamic driving forces contributing towards binding.

5.3 Van't Hoff Plots

Isocratic experiments were carried out over a range of salt and temperature conditions as described in the experimental section and a VH analysis was carried out to determine the thermodynamics. Figures 3 and S1 show representative VH plots (ln k' versus 1/T) for the retention data of mAbs A and C, respectively, on the three resin systems. Representative data for the lower and higher salt regimes are presented at the top and bottom portions of the figure. The data were fit to the quadratic VH equation (Eq. 6) using Matlab R2019b to determine the parameters a, b and c with a maximum fitting error of 10% in a 95% confidence interval and the resulting curves are

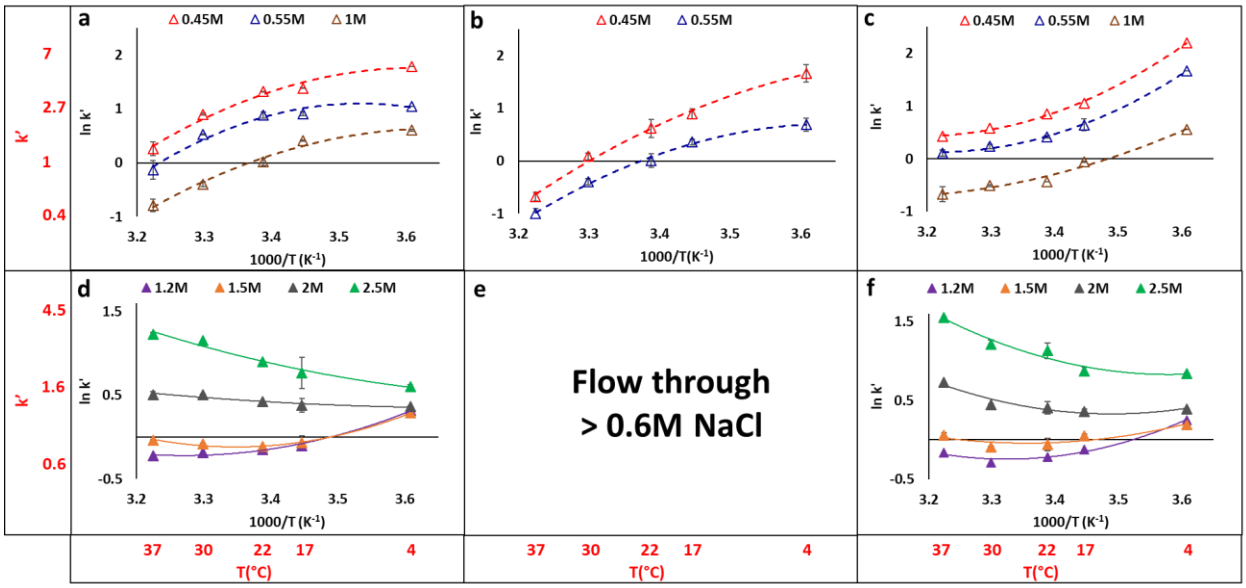

Figure 3. Non-linear van't Hoff plots for adsorption of mAb A on (a,d) Capto MMC, (b,e) Nuvia cPrime and (c,f) Capto MMC ImpRes at different salt concentrations. Curves generated by fitting the quadratic VH equation are presented as dotted lines for low salt regime (0.45, red; 0.55, blue; 1 M, brown; NaCl) and solid lines for high salt regime (1.2, violet; 1.5, orange; 2, grey; and 2.5 M, green; NaCl).

also presented in the Figures. As can be seen, the data were accurately represented by the non-linear VH plots. The non-linearity of the VH plots can be a result of multiplicity of interactions further indicating dependence of enthalpy and entropy of binding on temperature in the temperature range studied [31–33,43]. While non-linear VH plots can arise from both changes in thermodynamics as well as changes in phase ratio, in these MM systems under investigation it is unlikely that there are any phase ratio changes that are responsible for this non-linearity.

As can be seen in the Figures, at all temperatures, the retention decreased with salt in the lower salt regime and increased with salt in the higher salt regime. Further, in the low salt regime, for both mAbs, while the retention decreased with increasing temperature on all MM CEX systems, the curvature behavior was different. For example, the VH plots for mAb A were all concave downwards for Capto MMC and Nuvia cPrime (Figure 3a,b) while being consistently concave upwards for Capto MMC ImpRes (Figure 3c). The VH plots for mAb C (Figure S1a,b,c) in general exhibited the same curvature trends as observed for mAb A. The differences in curvature of these plots will be discussed in the next section on the VH analysis.

In the high salt regime, the binding behavior of mAb A in the Capto MMC and Capto MMC ImpRes systems were similar, with a strong temperature dependence only seen at the upper end of the high salt regime (e.g. 2.5 M NaCl). On the other hand, mAb C was weakly retained in

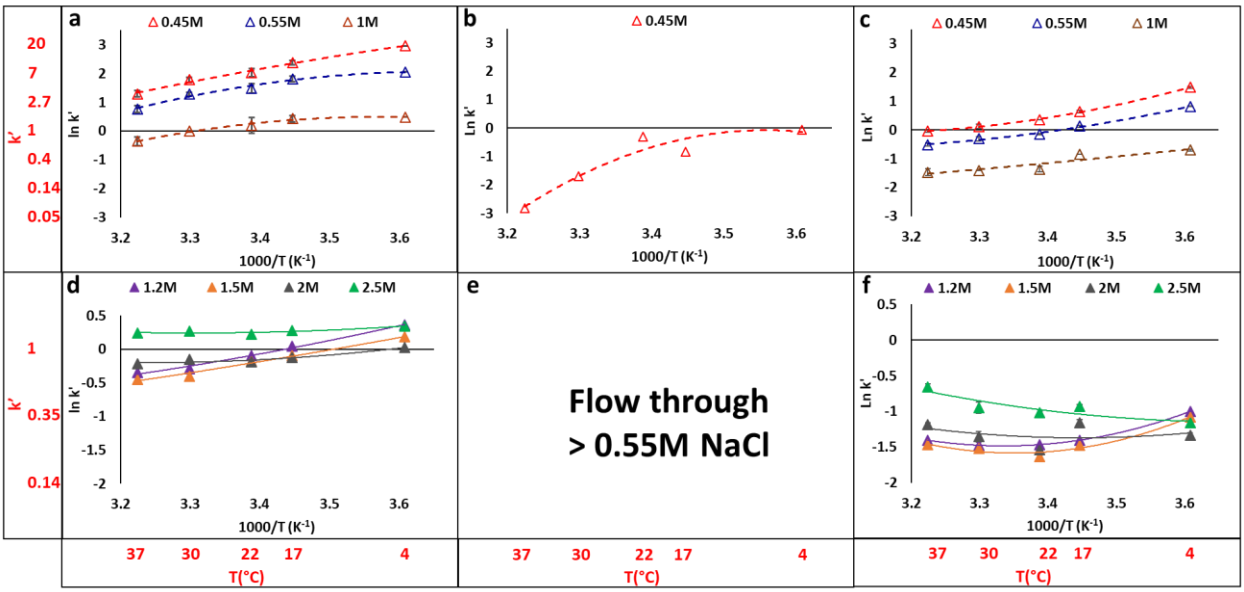

Figure S1. Non-linear van't Hoff plots for adsorption of mAb C on (a,d) Capto MMC, (b,e) Nuvia cPrime and (c,f) Capto MMC ImpRes at different salt concentrations. Curves generated by fitting the quadratic VH equation are presented as dotted lines for low salt regime (0.45, red; 0.55, blue; 1 M, brown; NaCl) and solid lines for high salt regime (1.2, violet; 1.5, orange; 2, grey; and 2.5 M, green; NaCl).

both Capto resin systems at the higher salt conditions and showed minimal temperature dependence (Figure S1d,f). For the Nuvia resin, there was minimal or no retention under all high salt conditions. The increased retention with increasing temperature observed with mAb A in the Capto resin systems at high salt is similar to that previously reported in some HIC systems [31,32,44]. While the data trends and the observed differences in curvature in the VH plots were quite interesting, it was also important to determine the enthalpic and entropic contributions towards these interactions in order to provide additional information.

5.4 Van't Hoff Analysis

As described in the previous section, the data from the VH plots (Figures 3 and S1) were fit to the quadratic VH equation (Eq. 6) using Matlab R2019b to determine the parameters a, b and c. The enthalpic (ΔH_{ads}) and entropic ($-T\Delta S_{ads}$) components were then calculated using equations 6-9 and are presented in the top and bottom portions, respectively, of Figures 4 and S2. To facilitate the discussion, a representative salt concentration from the low (0.45 M NaCl) and high salt (2.5 M NaCl) regimes are presented as well as an intermediate salt condition (1.2 M NaCl). As can be seen in Figure 4a,b,c, the enthalpic contribution to the binding of mAb A to the MM CEX resins was dependent on temperature for all the resin systems. In the low salt regime, the results indicated that while the binding was enthalpically driven in all cases, the trends with temperature were

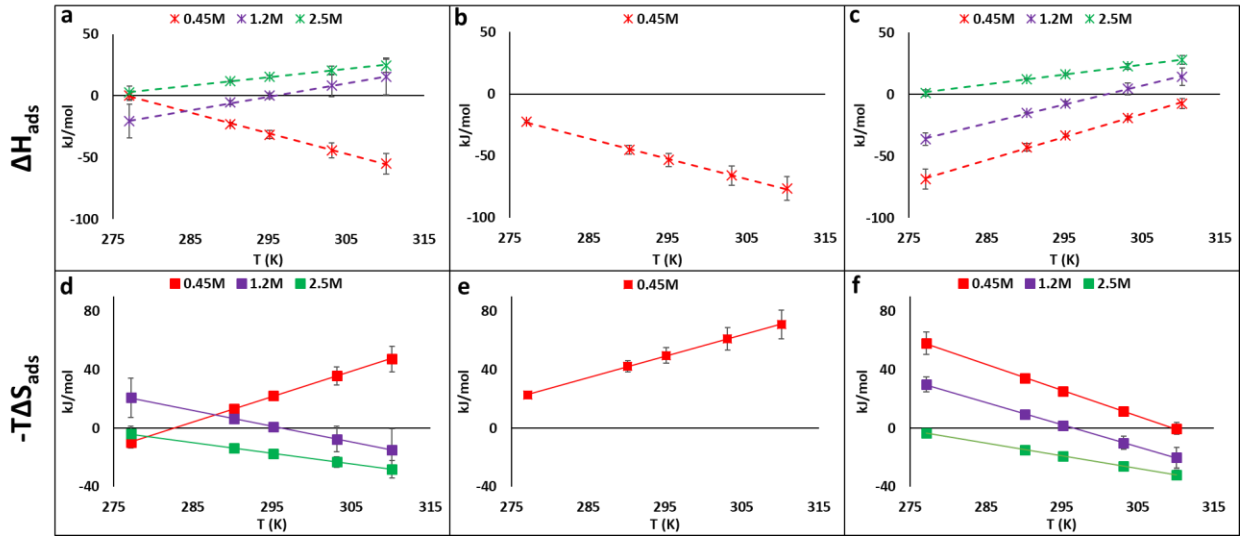

Figure 4. Enthalpic (top) and entropic (bottom) contributions at different temperatures (278, 290, 295, 303 and 310 K) and salt concentrations (0.45, red; 1.2, violet; and 2.5 M, green; NaCl) for binding of mAb A on (a,d) Capto MMC, (b,e) Nuvia cPrime and (c,f) Capto MMC ImpRes.

different, with the favorable enthalpic contributions increasing with temperature for Capto MMC and Nuvia cPrime systems and decreasing for Capto MMC ImpRes. In the high salt regime, the trends for mAb A were very similar for both Capto systems, with the favorable enthalpic component consistently decreasing with temperature at all salt concentrations (Figure 4a,c). Further, at the highest salt (2.5 M NaCl) the enthalpic contributions were consistently unfavorable for mAb A. For the Nuvia resin, the mAb A was weakly retained at salt concentrations above 0.45 M NaCl, limiting our analysis to this relatively low salt concentration.

Interestingly, the enthalpic trends observed for mAb C on the three resins at various salt concentrations (Figure S2a,b,c) were in general quite similar to those observed with mAb A. For Capto MMC, the changes in enthalpic trends seen for mAbs A and C at different salt concentrations could potentially indicate shifts in the preferred binding regions on the mAb surface for interacting with this resin.

The entropic contributions ($-T\Delta S_{ads}$) to the binding of mAb A to the MM CEX resins (Figure 4d,e,f) exhibited the opposite trends with temperature as were seen with the enthalpy, indicating enthalpy-entropy compensation [31,37,45,46]. In the low salt regime (0.45 M NaCl), the entropic contribution for binding was unfavorable for all the MM CEX resins, except at very low temperature (278 K) on Capto MMC resin, where it was favorable. While the favorable entropic component decreased (positive slope) with temperature for Capto MMC and Nuvia

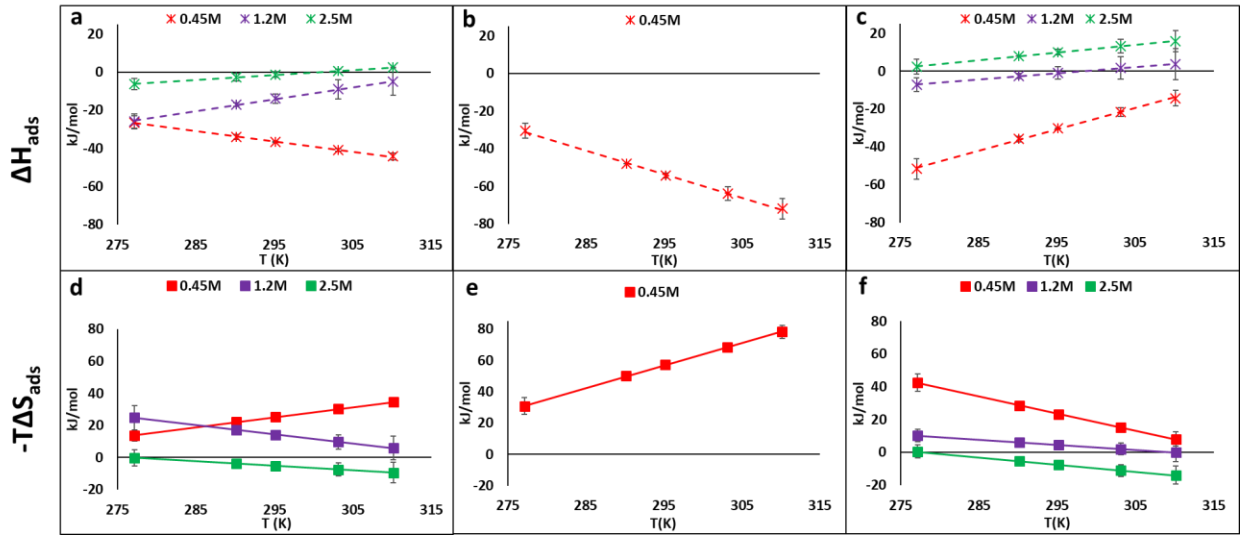

Figure S2. Enthalpic (top) and entropic (bottom) contributions at different temperatures (278, 290, 295, 303 and 310 K) and salt concentrations (0.45, red; 1.2, violet; and 2.5 M, green; NaCl) for binding of mAb C on (a,d) Capto MMC, (b,e) Nuvia cPrime and (c,f) Capto MMC ImpRes.

cPrime systems, it increased for the Capto MMC ImpRes resin. On the other hand, in the high salt regime, while we were unable to determine the entropic component in the Nuvia system due to weak retention of mAb A, the entropic trends were similar for the two Capto resins, with both exhibiting an increase in favorable entropy (negative slope) with temperature. Further, for mAb A the binding was completely entropically dominated at the highest salt (2.5 M NaCl) in both resins. As was observed with the enthalpy, the entropic trends at different conditions for mAb C (Figure S2d,e,f) were in general similar to those observed for mAb A (Figure 4d,e,f).

It's interesting to note that in the low salt regime, favorable enthalpic and unfavorable entropic contributions were observed for the binding of mAbs on all three MM CEX resin systems (Figures 4 and S2). The adsorption of proteins to MM resins can be driven by a complex combination of electrostatic, hydrophobic, H-bonding, van der Waals, pi-cation and/or aromatic interactions. Previous studies on microcalorimetric evaluation of protein binding to IEX systems have shown that the attractive electrostatic interactions are the major contributors towards favorable enthalpic contributions [47]. Since the binding of both mAbs on all MM resins decreased with increasing salt concentration in this low salt regime, the electrostatic interactions are likely also playing an important role here with the MM systems.

Interestingly, while the favorable enthalpic contributions increased with temperature for Nuvia cPrime and Capto MMC, they decreased for the Capto MMC ImpRes resin (Figures 4a,c

and S2a,c). These opposing trends for the Capto systems at these lower salt conditions may be due in part to differences in the resulting electrostatic potential presented by these resins at the two ligand densities. While the salt may be more effective at charge screening on the lower ligand density Capto MMC ImpRes, the higher density Capto MMC surface may have relatively lower charge screening while also exhibiting higher hydrophobicity. In fact, the increasing favorable enthalpic trend with temperature seen with Capto MMC has also been observed in some HIC systems where van der Waals interactions play an important role [31,48]. On the other hand, the enthalpy dependence on temperature observed with Capto MMC ImpRes is similar to that seen in IEX systems [49], where the decreasing strength of electrostatic interactions at elevated temperatures was indicative of decreasingly favorable enthalpic contributions. These results indicate that even though the binding was enthalpically driven for mAbs on the three MM CEX resins in the low salt regime, they likely interacted with different binding mechanisms which will be explored below when discussing the heat capacity data.

In contrast to the low salt conditions, the enthalpic contributions became less favorable and the binding was increasingly entropically driven on both Capto systems in the high salt regime (Figures 4 and S2). The decreasing favorable enthalpic contributions is likely due to the screening of electrostatic interactions at the higher salt concentrations. At the highest salt condition (2.5 M NaCl) the entropic contributions were observed to be favorable for both mAbs and Capto systems, indicating that hydrophobic interactions were very likely playing an important role in binding. It is well established that while the release of water molecules (desolvation) during binding results in a favorable entropic contribution, this disruption of well-ordered water structure also can lead to unfavorable enthalpy changes, trends observed in both figures. The observed increase in the entropic driving force with increasing temperature on both Capto resins, also supports desolvation

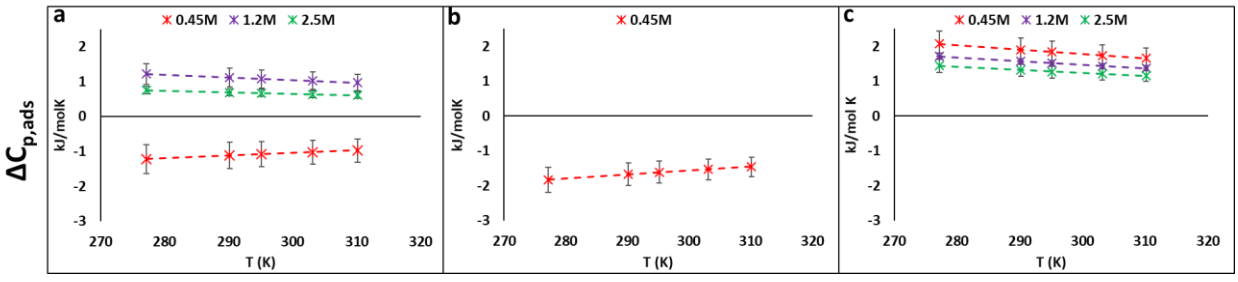

Figure 5. Heat capacity change upon adsorption of mAb A on (a) Capto MMC, (b) Nuvia cPrime and (c) Capto MMC ImpRes at different temperatures (278, 290, 295, 303 and 310 K) and salt concentrations (0.45, red; 1.2, violet; and 2.5 M, green; NaCl).

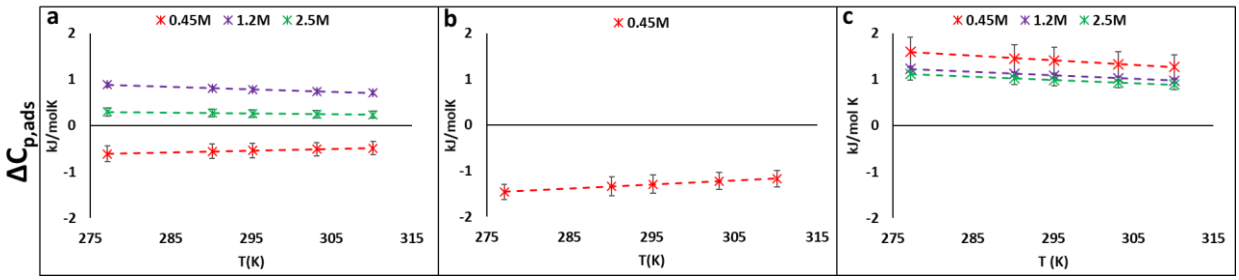

Figure S3. Heat capacity change upon adsorption of mAb C on (a) Capto MMC, (b) Nuvia cPrime and (c) Capto MMC ImpRes at different temperatures (278, 290, 295, 303 and 310 K) and salt concentrations (0.45, red; 1.2, violet; and 2.5 M, green; NaCl).

playing an important role here. This temperature behavior has also been observed in HIC systems [37,39,44] where desolvation entropy was deemed important. Finally, while unfavorable configurational entropy can sometimes play a role in protein binding, the fact that the entropy was consistently favorable at the high salt conditions again supports desolvation as a major driver. Clearly, the energetic trends for mAb interactions with the MM resins at low and high salt conditions are indicative of different binding mechanisms occurring in these two regimes.

The heat capacity values were also obtained from the VH analysis and are presented in Figures 5 and S3. As can be seen, the heat capacities showed minimal dependence on temperature. Further, while modest negative values for $\Delta C_{P,ads}$ were obtained for both mAbs on Capto MMC and Nuvia cPrime at low salt, the heat capacities were positive at the higher salts for Capto MMC (note: weak retention of mAbs at higher salts on Nuvia cPrime, limited our analysis for this resin to the low salt condition. In contrast, the $\Delta C_{P,ads}$ values for Capto MMC ImpRes were consistently positive for both mAbs in the two salt regimes. Reports in the literature have indicated that while negative heat capacity values are indicative of desolvation of the polar/charged residues upon binding, the dehydration of non-polar groups result in positive $\Delta C_{P,ads}$ values [31,50]. In addition, protein conformational changes upon binding can lead to exposure of buried non-polar groups, potentially contributing towards positive $\Delta C_{P,ads}$ values [32]. The negative values in the low salt regime for the binding of both mAbs in the Capto MMC and Nuvia cPrime systems indicate that desolvation of polar groups may be playing a role in binding, supporting our contention that the electrostatic interactions are playing a major role in binding. In contrast, the results with Capto MMC ImpRes at the low salt condition indicate that desolvation of non-polar groups may be playing an important role which may be due to a different preferred binding region for this lower ligand density resin material. On the other hand, at the high salt conditions where the hydrophobic

interactions were more important for binding, the positive values for both Capto systems are likely indicative of dehydration of the non-polar residues. These heat capacity results in concert with the thermodynamic data discussed above, shed light on the dominant modes of interactions of these mAbs in the MM CEX systems in the two salt regimes as well as subtle differences between the different resin systems.

6 Conclusions

In this study, the binding of two industrial mAbs that had previously been shown to exhibit unique selectivity patterns on MM CEX resins was evaluated from a thermodynamic perspective. Isocratic chromatographic experiments were carried out on these resins (Capto MMC, Nuvia cPrime and Capto MMC ImpRes) over a range of temperature and salt conditions to generate the data for the non-linear VH analysis. The retention data were evaluated in both the low (0.45 to 1.0 M NaCl) and high salt (1.2 to 2.5 M NaCl) regimes. While the retention at room temperature of the two mAbs decreased with salt for all the resins in the low salt regime, the retention increased at elevated salts on the two Capto systems. The Nuvia cPrime resin exhibited a stronger dependence on salt than the Capto systems in the low salt regime, while having minimal retention above 0.6 M NaCl, likely due to decreased contributions from the sterically inaccessible aromatic moiety on the ligand. These retention patterns with salt indicate a shift from electrostatically driven to more hydrophobic interactions in the Capto resins when transitioning from the low to the higher salt regime.

The retention data at various temperatures were used to generate VH plots which were clearly non-linear and which were well fit to the quadratic form of VH equation. This indicated that multiple interactions were likely involved in the binding. In the low salt regime, the retention of both mAbs decreased with increasing temperature and the VH plots were concave downward on the Capto MMC and Nuvia cPrime resins while being concave upward on the Capto MMC ImpRes system. Further, this difference in curvature was more pronounced with the more hydrophobic mAb A than with mAb C. In the high salt regime, while the retention of mAb A increased with temperature on both Capto resins, mAb C exhibited minimal temperature dependence.

The fits of the data to the quadratic VH equation were used to provide insights into the enthalpic and entropic contributions to binding under different conditions as well as the heat capacities. In the low salt regime, while the entropic contributions were unfavorable, the enthalpy was favorable for all resin systems with different temperature trends observed. Interestingly, while increasingly favorable enthalpic contributions with increasing temperature were observed with the Capto MMC and Nuvia cPrime systems, the favorable enthalpy was seen to decrease with increasing temperature for Capto MMC ImpRes. These enthalpic trends with temperature indicate different mechanisms involved in binding in these MM systems at low salt. On the other hand, at the high salt condition (2.5 M NaCl), binding of both mAbs on the two Capto resins was consistently entropically driven, indicating that desolvation was the major driver for binding.

Clearly, the complexity of these mAb biomolecules makes it difficult to directly connect this thermodynamic information with their specific molecular interactions with the multimodal resins. However, some insights were obtained by examining the heat capacity trends. For example, the negative heat capacities at low salts obtained with the Capto MMC and Nuvia cPrime resins indicated that desolvation of polar/charged groups on the mAb surfaces were potentially playing an important role. In contrast, the positive heat capacity values at low salts with the lower ligand density Capto MMC ImpRes resin, may be indicative of a contribution from desolvation of non-polar groups. Finally, in the high salt regime, the positive heat capacity values in concert with the entropic driving forces were indicative of desolvation of non-polar groups being an important driver for the binding of both mAbs on the two Capto systems.

The work in this paper demonstrates clear differences in the thermodynamic behavior for the three MM CEX resin systems in two salt regimes. It is expected that these thermodynamic differences will be even more pronounced in multimodal anion exchange systems, where increased retention with salt has been observed even at lower salts. Further, the difference in energetics with temperature for these two mAbs raises questions about the distribution and types of binding regions on these protein surfaces. Future work will focus on evaluation of the preferred regions on the mAb surfaces involved in binding to the resins using covalent cross-linking and mass spectrometry analysis as well as MD simulations. This will enable us to make more direct connection between the thermodynamic trends and molecular interactions involved with these particular binding regions and chromatographic surfaces.

7 Acknowledgements

The authors would like to acknowledge Mayank Vats for helpful discussion. This material is based upon work supported by the National Science Foundation (Grant number CBET 1704745) and Merck & Co., Inc. (Kenilworth, NJ, 07033, USA).

8 References

[1] Y. Tao, G. Carta, G. Ferreira, D. Robbins, Adsorption of deamidated antibody variants on macroporous and dextran-grafted cation exchangers: I. Adsorption equilibrium, J. Chromatogr. A. 1218 (2011) 1519–1529. doi:10.1016/j.chroma.2011.01.049.

[2] Y. Lu, B. Williamson, R. Gillespie, Recent Advancement in Application of Hydrophobic Interaction Chroma-tography for Aggregate Removal in Industrial Purification Process, Curr Pharm Biotechnol. 10 (2009) 427-433. doi: 10.2174/138920109788488897.

[3] W.R. Melander, Z. El Rassi, C. Horváth, Interplay of hydrophobic and electrostatic interactions in biopolymer chromatography : Effect of salts on the retention of proteins, J. Chromatogr. A. 469 (1989) 3–27. doi:10.1016/S0021-9673(01)96437-4.

[4] S.C. Burton, N.W. Haggarty, D.R.K. Harding, One step purification of chymosin by mixed mode chromatography, Biotechnol. Bioeng. 56 (1997) 45–55. doi:10.1002/(SICI)1097-0290(19971005)56:1<45::AID-BIT5>3.0.CO;2-V.

[5] S.C. Burton, D. Roger, K. Harding, High-density ligand attachment to brominated allyl matrices and application to mixed mode chromatography of chymosin, J. Chromatogr. A. 775 (1997) 39-50. doi.org/10.1016/S0021-9673(97)00515-3.

[6] B.-L. Johansson, M. Belew, S. Eriksson, G. Glad, O. Lind, J.-L. Maloisel, N. Norrman, Preparation and characterization of prototypes for multi-modal separation media aimed for capture of negatively charged biomolecules at high salt conditions, J. Chromatogr. A. 1016 (2003) 21–33. doi:10.1016/S0021-9673(03)01140-3.

[7] S. Ghose, B. Hubbard, S.M. Cramer, Protein interactions in hydrophobic charge induction chromatography (HCIC), Biotechnol. Prog. 21 (2005) 498–508. doi:10.1021/bp049712+.

[8] S.M. Cramer, M.A. Holstein, Downstream bioprocessing: recent advances and future

promise, Curr. Opin. Chem. Eng. 1 (2011) 27–37. doi:10.1016/j.coche.2011.08.008.

[9] M.A. Holstein, S. Parimal, S.A. McCallum, S.M. Cramer, Mobile phase modifier effects in multimodal cation exchange chromatography, Biotechnol. Bioeng. 109 (2012) 176–186. doi:10.1002/bit.23318.

[10] J. Woo, S. Parimal, M.R. Brown, R. Heden, S.M. Cramer, The effect of geometrical presentation of multimodal cation-exchange ligands on selective recognition of hydrophobic regions on protein surfaces, J. Chromatogr. A. 1412 (2015) 33–42. doi:10.1016/j.chroma.2015.07.072.

[11] J.A. Woo, H. Chen, M.A. Snyder, Y. Chai, R.G. Frost, S.M. Cramer, Defining the property space for chromatographic ligands from a homologous series of mixed-mode ligands, J. Chromatogr. A. 1407 (2015) 58–68. doi:10.1016/j.chroma.2015.06.017.

[12] J. Robinson, M.A. Snyder, C. Belisle, J. Liao, H. Chen, X. He, Y. Xu, S.M. Cramer, Investigating the impact of aromatic ring substitutions on selectivity for a multimodal anion exchange prototype library, J. Chromatogr. A. 1569 (2018) 101–109. doi:10.1016/J.CHROMA.2018.07.049.

[13] W.K. Chung, Y. Hou, M. Holstein, A. Freed, G.I. Makhatadze, S.M. Cramer, Investigation of Protein Binding Affinity and Preferred Orientations in Ion Exchange Systems Using a Homologous Protein Library, J. Chromatogr. A. 1217 (2010) 191–198. doi:10.1016/j.chroma.2009.08.005.

[14] M.A. Holstein, S. Parimal, S.A. McCallum, S.M. Cramer, Effects of urea on selectivity and protein-ligand interactions in multimodal cation exchange chromatography, Langmuir. 29 (2013) 158–167. doi:10.1021/la302360b.

[15] M.A. Holstein, A.A.M. Nikfetrat, M. Gage, A.G. Hirsh, S.M. Cramer, Improving selectivity in multimodal chromatography using controlled pH gradient elution, J. Chromatogr. A. 1233 (2012) 152–155. doi:10.1016/j.chroma.2012.01.074.

[16] J. Robinson, D. Roush, S. Cramer, Domain contributions to antibody retention in multimodal chromatography systems, J. Chromatogr. A. 1563 (2018) 89–98. doi:10.1016/j.chroma.2018.05.058.

[17] J.R. Robinson, H.S. Karkov, J.A. Woo, B.O. Krogh, S.M. Cramer, QSAR models for prediction of chromatographic behavior of homologous Fab variants, Biotechnol. Bioeng. 114 (2017) 1231–1240. doi:10.1002/bit.26236.

[18] J. Robinson, D. Roush, S.M. Cramer, The effect of pH on antibody retention in multimodal cation exchange chromatographic systems, J. Chromatogr. A. 1617 (2020) 460838. doi:10.1016/j.chroma.2019.460838.

[19] C.L. Bilodeau, E.Y. Lau, D. Roush, S. Garde, S.M. Cramer, Formation of Ligand Clusters on Multimodal Chromatographic Surfaces, Langmuir. 35 (2019) 16770-16779. doi:10.1021/acs.langmuir.9b01925.

[20] S. Parimal, S. Garde, S.M. Cramer, Interactions of Multimodal Ligands with Proteins: Insights into Selectivity Using Molecular Dynamics Simulations, Langmuir. 31 (2015) 7512-7523. doi:10.1021/acs.langmuir.5b00236.

[21] K. Srinivasan, M. Sorci, L. Sejergaard, S. Ranjan, G. Belfort, S.M. Cramer, Protein Binding Kinetics in Multimodal Systems: Implications for Protein Separations, Anal. Chem. 90 (2018) 2609-2617. doi:10.1021/acs.analchem.7b04158.

[22] K. Srinivasan, S. Banerjee, S. Parimal, L. Sejergaard, R. Berkovich, B. Barquera, S. Garde, S.M. Cramer, Single Molecule Force Spectroscopy and Molecular Dynamics Simulations as a Combined Platform for Probing Protein Face-Specific Binding, Langmuir. 33 (2017) 53. doi:10.1021/acs.langmuir.7b03011.

[23] K. Srinivasan, S. Parimal, M.M. Lopez, S.A. McCallum, S.M. Cramer, Investigation into the molecular and thermodynamic basis of protein interactions in multimodal chromatography using functionalized nanoparticles, Langmuir. 30 (2014) 13205–13216. doi:10.1021/la502141q.

[24] B.K. Nfor, M. Noverraz, S. Chilamkurthi, P.D.E.M. Verhaert, L.A.M. van der Wielen, M. Ottens, High-throughput isotherm determination and thermodynamic modeling of protein adsorption on mixed mode adsorbents, J. Chromatogr. A. 1217 (2010) 6829–6850. doi:10.1016/j.chroma.2010.07.069.

[25] P. Gagnon, Monoclonal antibody purification with hydroxyapatite, N. Biotechnol. 25

(2009) 287–293. doi:10.1016/J.NBT.2009.03.017.

[26] L. Dattolo, E.L. Keller, G. Carta, pH transients in hydroxyapatite chromatography columns—Effects of operating conditions and media properties, J. Chromatogr. A. 1217 (2010) 7573–7578. doi:10.1016/J.CHROMA.2010.10.026.

[27] J. Chen, J. Tetrault, Y. Zhang, A. Wasserman, G. Conley, M. DiLeo, E. Haimes, A.E. Nixon, A. Ley, The distinctive separation attributes of mixed-mode resins and their application in monoclonal antibody downstream purification process, J. Chromatogr. A. 1217 (2010) 216–224. doi:10.1016/J.CHROMA.2009.09.047.

[28] L. Zhang, S. Bai, Y. Sun, Molecular dynamics simulation of the effect of ligand homogeneity on protein behavior in hydrophobic charge induction chromatography, J. Mol. Graph. Model. 28 (2010) 863–869. doi:10.1016/J.JMGM.2010.03.006.

[29] H.F. Tong, C. Cavallotti, S.J. Yao, D.Q. Lin, Molecular insight into protein binding orientations and interaction modes on hydrophobic charge-induction resin, J. Chromatogr. A. 1512 (2017) 34–42. doi:10.1016/j.chroma.2017.06.071.

[30] D.J. Roush, D.S. Gill, R.C. Willson, Anion-exchange chromatographic behavior of recombinant rat cytochrome b5: Thermodynamic driving forces and temperature dependence of the stoichiometric displacement parameter Z, J. Chromatogr. A. 653 (1993) 207–218. doi:10.1016/0021-9673(93)83176-S.

[31] H.C. Haidacher D., Vailaya A., Horváth C., Temperature effects in hydrophobic interaction chromatography, Proc. Natl. Acad. Sci. 93 (1996) 2290–2295.

[32] R. Ueberbacher, A. Rodler, R. Hahn, A. Jungbauer, Hydrophobic interaction chromatography of proteins: Thermodynamic analysis of conformational changes, J. Chromatogr. A. 1217 (2010) 184–190. doi:10.1016/j.chroma.2009.05.033.

[33] R.I. Boysen, Y. Wang, H.H. Keah, M.T.W. Hearn, Observations on the origin of the non-linear van't Hoff behaviour of polypeptides in hydrophobic environments, Biophys. Chem. 77 (1999) 79–97. doi:10.1016/S0301-4622(99)00002-2.

[34] F. Fang, M.-I. Aguilar, M.T.W. Hearn, Influence of temperature on the retention behaviour of proteins in cation-exchange chromatography, J. Chromatogr. A. 729 (1996) 49-66.

508 doi.org/10.1016/0021-9673(96)00008-8.

509 [35] F.Y. Lin, W.Y. Chen, M.T.W. Hearn, Thermodynamic analysis of the interaction between
510 proteins and solid surfaces: Application to liquid chromatography, J. Mol. Recognit. 15
511 (2002) 55–93. doi:10.1002/jmr.564.

512 [36] A. Vailaya, C. Horváth, Retention Thermodynamics in Hydrophobic Interaction
513 Chromatography, Ind. Eng. Chem. Res. 35 (1996) 2964-2981. doi.org/10.1021/ie9507437.

514 [37] W.Y. Chen, H.M. Huang, C.C. Lin, F.Y. Lin, Y.C. Chan, Effect of Temperature on
515 Hydrophobie Interaction between Proteins and Hydrophobic Adsorbents: Studies by
516 Isothermal Titration Calorimetry and the van't Hoff Equation, Langmuir. 19 (2003) 9395–
517 9403. doi:10.1021/la034783o.

518 [38] M.E. Thrash, J.M. Phillips, N.G. Pinto, An Analysis of the Interactions of BSA with an
519 Anion-Exchange Surface Under Linear and Non-Linear Conditions, Adsorption. 10 (2004)
520 299-307. doi.org/10.1007/s10450-005-4815-0.

521 [39] A.C. Dias-Cabral, J.A. Queiroz, N.G. Pinto, Effect of salts and temperature on the
522 adsorption of bovine serum albumin on polypropylene glycol-Sepharose under linear and
523 overloaded chromatographic conditions, J. Chromatogr. A. 1018 (2003) 137–153.
524 doi:10.1016/j.chroma.2003.07.010.

525 [40] K.J. Snyder Lloyd, Introduction to Modern Liquid Chromatography, John Wiley & Sons,
526 Inc. 2nd ed. 1979.

527 [41] F.S. Marques, G.L. Silva, M.E. Thrash, A.C. Dias-Cabral, Lysozyme adsorption onto a
528 cation-exchanger: Mechanism of interaction study based on the analysis of retention
529 chromatographic data, Colloid Surface B. 122 (2014) 801–807.
530 doi:10.1016/j.colsurfb.2014.08.024.

531 [42] D. Wu, R.R. Walters, Effects of stationary phase ligand density on high-performance ion-
532 exchange chromatography of proteins, J. Chromatogr. A. (1992). doi:10.1016/0021-
533 9673(92)85108-6.

534 [43] M. Tanase, A. Soare, V. David, S.C. Moldoveanu, Sources of Nonlinear van't Hoff
535 Temperature Dependence in High-Performance Liquid Chromatography, ACS Omega, 4

(2019) 19808-19817. doi:10.1021/acsomega.9b02689.

[44] A.S. Ferreira, J. Phillips, J.A. Queiroz, N.G. Pinto, The effects of ligand chain length , salt concentration and temperature on the adsorption of bovine serum albumin onto polypropyleneglycol – Sepharose, 616 (2005) 606–616. doi:10.1002/bmc.487.

[45] L. Liu, C. Yang, Q.-X. Guo, A study on the enthalpyentropy compensation in protein unfolding, Biophys Chem. 84 (2000) 239-251. doi: 10.1016/s0301-4622(00)00130-7.

[46] N. Morin, Y.C. Guillaume, E. Peyrin, J.-C. Rouland, Peculiarities of an imidazole derivative retention mechanism in reversed-phase liquid chromatography: b-cyclodextrin concentration and temperature considerations, J. Chromatogr. A. 808 (1998) 51-60. doi.org/10.1016/S0021-9673(98)00107-1.

[47] W.-Y. Chen, Z.-C. Liu, P.-H. Lin, C.-I. Fang, S. Yamamoto, The hydrophobic interactions of the ion-exchanger resin ligands with proteins at high salt concentrations by adsorption isotherms and isothermal titration calorimetry, Sep. Purif. Technol. 54 (2007) 212–219. doi:10.1016/J.SEPPUR.2006.09.008.

[48] T.W. Perkins, D.S. Mak, T.W. Root, E.N. Lightfoot, Protein retention in hydrophobic interaction chromatography: Modeling variation with buffer ionic strength and column hydrophobicity, J. Chromatogr. A. 766 (1997) 1–14. doi:10.1016/S0021-9673(96)00978-8.

[49] T.W. Hutchens, T.-T. Yip, Protein Interactions With Surface-Immobilized Metal Ions: Structure-Dependent Variations in Affinity and Binding Capacity with Temperature and Urea Concentration, J. Inorg. Biochem. 42 (1991) 105-118. doi: 10.1016/0162-0134(91)80037-i.

[50] N. V. Prabhu, K.A. Sharp, Heat Capacity in Proteins, Annu. Rev. Phys. Chem. 56 (2005) 521–548. doi:10.1146/annurev.physchem.56.092503.141202.

Figure Captions

Figure 1: (a) Chromatographic retention of mAbs A (purple) and C (blue) on multimodal cation exchange chromatography systems and structures of the (b) Capto and (C) Nuvia cPrime ligand head groups (numbers in parenthesis indicate the corresponding ligand densities on the

564 chromatographic resin surfaces). Capto MMC and Capto MMC ImpRes resins have the same
565 ligand head group with different surface ligand density. Linear salt gradients were from 0 to 1M
566 NaCl, 40 CV, pH 6. Retention data reproduced from ref [16].

567 Figure 2: Ln k' vs Ln Cs plots for retention of mAbs A (purple) and C (blue) on (a) Capto MMC,
568 (b) Nuvia cPrime and (c) Capto MMC ImpRes at room temperature (295 K).

569 Figure 3: Non-linear van't Hoff plots for adsorption of mAb A on (a,d) Capto MMC, (b,e) Nuvia
570 cPrime and (c,f) Capto MMC ImpRes at different salt concentrations. Curves generated by fitting
571 the quadratic VH equation are presented as dotted lines for the low salt regime (0.45, red; 0.55,
572 blue; 1 M, brown; NaCl) and solid lines for the high salt regime (1.2, violet; 1.5, orange; 2, grey;
573 and 2.5 M, green; NaCl).

574 Figure 4: Enthalpic (top) and entropic (bottom) contributions at different temperatures (278, 290,
575 295, 303 and 310 K) and salt concentrations (0.45, red; 1.2, violet; and 2.5 M, green; NaCl) for
576 binding of mAb A on (a,d) Capto MMC, (b,e) Nuvia cPrime and (c,f) Capto MMC ImpRes.

577 Figure 5: Heat capacity change upon adsorption of mAb A on (a) Capto MMC, (b) Nuvia cPrime
578 and (c) Capto MMC ImpRes at different temperatures (278, 290, 295, 303 and 310 K) and salt
579 concentrations (0.45, red; 1.2, violet; and 2.5 M, green; NaCl).

580 Figure S1: Non-linear van't Hoff plots for adsorption of mAb C on (a,d) Capto MMC, (b,e) Nuvia
581 cPrime and (c,f) Capto MMC ImpRes at different salt concentrations. Curves generated by fitting
582 the quadratic VH equation are presented as dotted lines for the low salt regime (0.45, red; 0.55,
583 blue; 1 M, brown; NaCl) and solid lines for the high salt regime (1.2, violet; 1.5, orange; 2, grey;
584 and 2.5 M, green; NaCl).

585 Figure S2: Enthalpic (top) and entropic (bottom) contributions at different temperatures (278, 290,
586 295, 303 and 310 K) and salt concentrations (0.45, red; 1.2, violet; and 2.5 M, green; NaCl) for
587 binding of mAb C on (a,d) Capto MMC, (b,e) Nuvia cPrime and (c,f) Capto MMC ImpRes.

588 Figure S3: Heat capacity change upon adsorption of mAb C on (a) Capto MMC, (b) Nuvia cPrime
589 and (c) Capto MMC ImpRes at different temperatures (278, 290, 295, 303 and 310 K) and salt
590 concentrations (0.45, red; 1.2, violet; and 2.5 M, green; NaCl).